

Original citation:

Gomes, M. Gabriela M., Lipsitch, Marc, Wargo, Andrew R., Kurath, Gael, Rebelo, Carlota, Medley, Graham and Coutinho, Antonio. (2014) A missing dimension in measures of vaccination impacts. PLoS Pathogens, Volume 10 (Number3). Article Number e1003849.

Permanent WRAP url:

<http://wrap.warwick.ac.uk/59713>

Copyright and reuse:

The Warwick Research Archive Portal (WRAP) makes this work of researchers of the University of Warwick available open access under the following conditions.

This article is made available under Creative Commons CC0 1.0 Universal (CC0 1.0) Public Domain Dedication and may be reused according to the conditions of the license. For more details see <https://creativecommons.org/publicdomain/zero/1.0/>

A note on versions:

The version presented in WRAP is the published version, or, version of record, and may be cited as it appears here.

For more information, please contact the WRAP Team at: publications@warwick.ac.uk

warwick**publications**wrap

highlight your research

<http://wrap.warwick.ac.uk/>

Opinion

A Missing Dimension in Measures of Vaccination Impacts

M. Gabriela M. Gomes^{1*}, Marc Lipsitch², Andrew R. Wargo³, Gael Kurath⁴, Carlota Rebelo⁵, Graham F. Medley⁶, Antonio Coutinho¹

1 Instituto Gulbenkian de Ciência, Oeiras, Portugal, **2** Center for Communicable Disease Dynamics, Harvard School of Public Health, Boston, Massachusetts, United States of America, **3** Virginia Institute of Marine Science, College of William and Mary, Gloucester Point, Virginia, United States of America, **4** U.S. Geological Survey, Western Fisheries Research Center, Seattle, Washington, United States of America, **5** Faculdade de Ciências de Lisboa e Centro de Matemática e Aplicações Fundamentais, Campo Grande, Lisboa, Portugal, **6** School of Life Sciences and WIDER, University of Warwick, Coventry, United Kingdom

Immunological protection, acquired from either natural infection or vaccination, varies among hosts, reflecting underlying biological variation and affecting population-level protection. Owing to the nature of resistance mechanisms, distributions of susceptibility and protection entangle with pathogen dose in a way that can be decoupled by adequately representing the dose dimension. Any infectious processes must depend in some fashion on dose, and empirical evidence exists for an effect of exposure dose on the probability of transmission to mumps-vaccinated hosts [1], the case-fatality ratio of measles [2], and the probability of infection and, given infection, of symptoms in cholera [3]. Extreme distributions of vaccine protection have been termed leaky (partially protects all hosts) and all-or-nothing (totally protects a proportion of hosts) [4]. These distributions can be distinguished in vaccine field trials from the time dependence of infections [5]. Frailty mixing models have also been proposed to estimate the distribution of protection from time to event data [6,7], although the results are not comparable across regions unless there is explicit control for baseline transmission [8]. Distributions of host susceptibility and acquired protection can be estimated from dose-response data generated under controlled experimental conditions [9–11] and natural settings [12,13]. These distributions can guide research on mechanisms of protection, as well as enable model validity across the entire range of transmission intensities. We argue for a shift to a dose-dimension paradigm in infectious disease science and community health.

Natural Transmission

We consider a minimal susceptible (S) and infected (I) model [14] of pathogen transmission in a host population to explore population effects of protection conferred by a vaccine (or other preventive measure, such as symbionts) against infection, under different assumptions about how this is distributed among

individuals. We consider that infection is lifelong, and that there is no naturally acquired immunity.

Vaccines that provide leaky protection against infection act by reducing susceptibility to a factor σ that is distributed among individuals according to a probability density function $q(x)$, where $0 < x < 1$. Denoting by $i_v(x)$ the densities of hosts who are vaccinated and have susceptibility factor x , the integral $I_v = \int_0^1 i_v(x) dx$ represents the proportion of hosts who are infected despite being vaccinated. Assuming no effect on infectiousness, the per capita rate of infection among totally susceptible individuals is given by $\lambda = \beta(I + I_v)$, where β is the effective contact rate.

Figure 1A shows, for the distributions $q(x)$ represented on the right, equilibrium curves describing prevalence of infection versus transmission intensity measured by R_0 , the basic reproduction number. The curves for extreme cases of vaccines that confer equal protection to all or total protection to some and none to others are depicted by the higher (red) and lower (blue) curves, respectively. Intermediate curves represent scenarios in which susceptibility follows a beta distribution with fixed mean and increasing variance from top to bottom. Prevalence curves become shallower with heterogeneity and converge to the same level as transmission increases, except in the all-or-nothing extreme, in which the

prevalence cannot surpass the susceptible fraction, irrespective of transmission intensity. Although the impact of protection appears to increase with polarization of effects, the endemic curves do not converge uniformly to their all-or-nothing homologue. In the absence of unequivocal empirical evidence for the idealized all-or-nothing mode of action, we suggest modifying the terminology to include polarized distributions more generally.

This illustration indicates that the distribution of vaccine effects among individuals is a major determinant of population-level impact and should be considered in evaluation. Specifically, the more homogeneously a vaccine acts, the lower its impact on disease transmission. Measures based on multipopulation study designs, spanning a range of transmission intensities, enable the inference of such distributions.

Experimental Challenge

Infection in a controlled experimental setting is modeled by describing infected proportions in terms of challenge dose. Adopting standard formulations [15–17], the mean number of infecting pathogens is pd , where d is the number of pathogens challenging the host, and p is the probability of infection for each pathogen; the number of infecting pathogens per host has a Poisson distribution with mean pd . In the homogeneous case, the probability

Citation: Gomes MGM, Lipsitch M, Wargo AR, Kurath G, Rebelo C, et al. (2014) A Missing Dimension in Measures of Vaccination Impacts. *PLoS Pathog* 10(3): e1003849. doi:10.1371/journal.ppat.1003849

Editor: Glenn F. Rall, The Fox Chase Cancer Center, United States of America

Published: March 6, 2014

This is an open-access article, free of all copyright, and may be freely reproduced, distributed, transmitted, modified, built upon, or otherwise used by anyone for any lawful purpose. The work is made available under the Creative Commons CC0 public domain dedication.

Funding: This research was supported by the Portuguese Foundation for Science and Technology (FCT), the European Commission (EC-ICT-231807). CR was supported by FCT, PEst, OE/MAT/UI0209/2011 and project PTDC/MAT/113383/2009. ML was supported by Award Number U54GM088558 from the National Institute of General Medical Sciences. The content is solely the responsibility of the authors and does not necessarily represent the official views of the National Institute of General Medical Sciences or the National Institutes of Health. The funders had no role in study design, data collection and analysis, decision to publish, or preparation of the manuscript.

Competing Interests: The authors have declared that no competing interests exist.

* E-mail: ggomes@igc.gulbenkian.pt

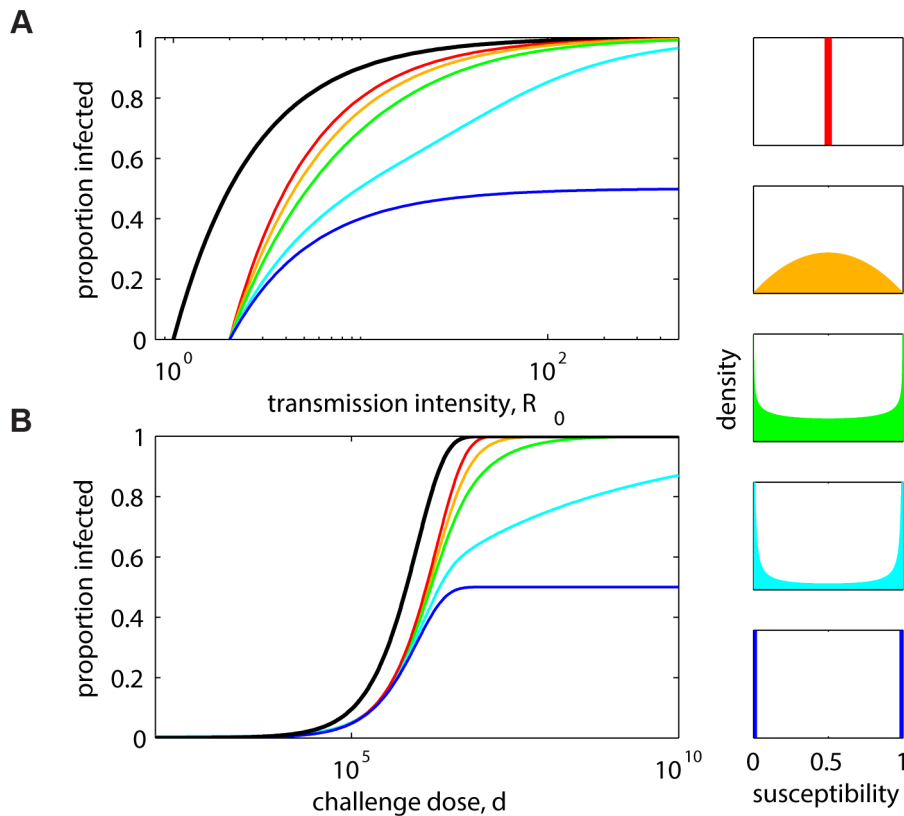


Figure 1. Decreasing infection with heterogeneity in host protection. (A) Equilibrium prevalence of infection under a pathogen transmission model in which an intervention (vaccine or symbiont) reduces host susceptibility to a factor that is distributed as specified. The model is formally represented by the rates of change in the proportions of the population that are susceptible and infected: $dS/dt = (1-v)\mu - \lambda S - \mu S$, $dI/dt = \lambda S - \mu I$, $ds_v(x)/dt = vq(x)\mu - x\lambda s_v(x) - \mu s_v(x)$, and $di_v(x)/dt = x\lambda s_v(x) - \mu i_v(x)$, where S and I are nonintervention, while $s_v(x)$ and $i_v(x)$ are intervention groups with susceptibility x distributed as $q(x)$ (right panels). Colored lines assume total intervention coverage ($v=1$), while the black line represents the scenario without intervention ($v=0$). (B) Dose-response curves expected from an experiment in which groups of naive (black) and intervention (colored) hosts are challenged with a range of pathogen doses, under a model in which the intervention reduces susceptibility to a factor that is distributed as in panels on the right. Models for infected proportions in nonintervention and intervention groups are formalized in a dose-response manner by $M = 1 - e^{-pd}$ and $M = 1 - \int_0^1 e^{-xpd} q(x) dx$, respectively, where d is the number of pathogens the host is challenged by and p is the probability of infection for each pathogen. Colored lines assume susceptibility factors distributed with mean 0.5 in all cases and variance 0 (red), 0.05 (orange), 0.1 (green), 0.2 (cyan), and 0.25 (blue). Red and blue at the extremes are discrete, while the intermediate cases are continuous beta distributions, with shape parameters a and b such that the mean is fixed, $E[\sigma] = a/(a+b) = 0.5$, and the variance, $\text{var}[\sigma] = ab/(a+b)^2(a+b+1)$, spans the range, $0 < \text{var}[\sigma] < 0.25$. Transmission models assume $\mu = 0.014$, and controlled infection models assume $p = 10^{-6}$. doi:10.1371/journal.ppat.1003849.g001

of a host remaining uninfected after pathogen challenge is the zero term of the distribution, leading to a probability of infection $M = 1 - e^{-pd}$, represented by the black curve in Figure 1B.

This model fails to fit many experimental data sets in which groups of hosts are exposed to varying doses of the pathogen, and the proportion infected in each group is calculated. In particular, the slope of the curve implied by this model is steeper than what is often observed. However, if individual hosts vary in their susceptibility to infection, a reduced slope arises. A simple model [11] assumes that the probability of each particle causing infection varies among hosts according to a beta distribution $q(x)$, akin to the vaccine protection factor above, resulting in the modified dose-response $M = 1 - \int_0^1 e^{-xpd} q(x) dx$.

Figure 1B illustrates dose-infectivity curves expected from an experiment in which groups of naive and vaccinated hosts are challenged with a range of pathogen doses under the distributions of protection described above, uncovering again a lack of uniform convergence to the all-or-nothing formulation.

We have adopted the same notation, $q(x)$, for susceptibility distributions in both natural transmission and experimental challenge settings to indicate the linkage between two arms of a unified study, as advocated here.

Classification of Intervention Effects

Experimental dose-infectivity curves provide information to infer the mode of

action of interventions, such as vaccines. Given the lack of uniform convergence to all-or-nothing as the leaky mode becomes increasingly polarized, we have classified beta distribution shapes according to polarization (Figure 2). The dashed line along the diagonal indicates the location of the symmetric distributions used in Figure 1, and the circles indicate the location of the extreme homogeneous (red) and all-or-nothing (blue) distributions. The power to identify polarized distributions is analyzed in Figure S1, focusing on a vicinity of the uniform shape (gray square), showing good discriminatory power in the region of parameter space where uncertainty is greatest. This analysis suggests a promising approach for classifying intervention effects in controlled experimental settings and using this as

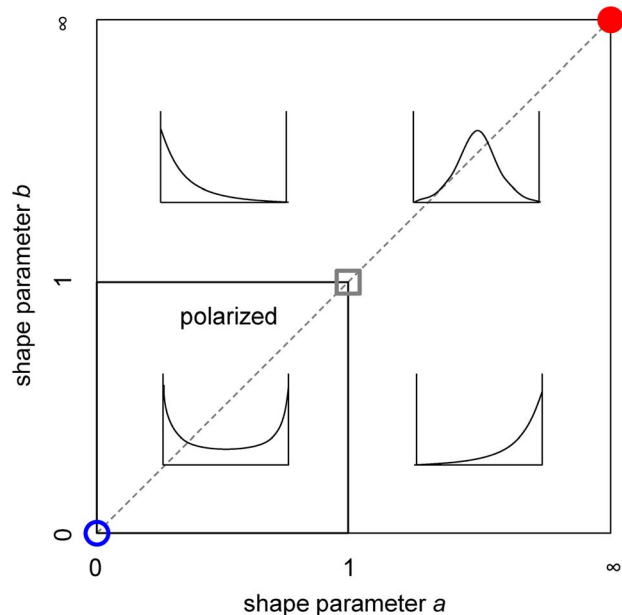


Figure 2. Shape classification in the terms of parameters a and b . Beta distributions are classified as: polarized if $a, b < 1$; symmetric if $a = b$ (gray dashed line), as in Figure 1; homogeneous in the limit $a, b \rightarrow \infty$ (red circle), as red in Figure 1; all-or-nothing in the limit $a, b \rightarrow 0$ (blue circle), as blue in Figure 1; and uniform if $a = b = 1$ (gray square). The power to identify polarized distributions is analyzed in a neighborhood of the uniform distribution (Figure S1). doi:10.1371/journal.ppat.1003849.g002

prior information for further study in natural settings [18].

Supporting Information

Figure S1 Power analysis to identify polarized intervention effects. Simulated sets of dose-infectivity data were generated and used to estimate model parameters (Figure S2), assuming the host susceptibility

of the intervention group described by a beta distribution, $q(x)$, with shape parameters positioned as a grid in a square neighborhood of the uniform distribution, $0.1 \leq a, b \leq 10$. The procedure was applied 100 times to each of 1,600 grip points, and the number of correct shape classifications into polarized ($a, b < 1$) versus non-polarized ($a > 1$ or $b > 1$) is represented. With 50

hosts per dose, the shape was identified with 95% accuracy in 57% of the simulated parameter space.

(TIFF)

Figure S2 Simulation and estimation experiment. A simulated set of dose-infectivity data was generated using models $M = 1 - e^{-pd}$ and $M = 1 - \int_0^1 e^{-xpd} q(x) dx$ for nonintervention and intervention groups, respectively, where d is the dose (simulated at 10^4 , 10^5 , 10^6 , 10^7 , 10^8 , 10^9 , and 10^{10}) and p is the probability of infection for each pathogen (simulated at 10^{-6}). The host susceptibility of the intervention group is described by a beta distribution, $q(x)$, with shape parameters $a = b = 0.5$. By fitting the models to the simulated data by a least squares procedure, we have estimated $p = 0.86 \times 10^{-6}$, $a = 0.42$, and $b = 0.18$. (A) The nonintervention arm of the experiment in black and the intervention arm in green. (B) Intervention effects' assumed distribution, shown as a dashed line, and the estimated distribution, represented as an unbroken line. This is an example in which a polarized intervention effect was estimated correctly.

(TIFF)

Acknowledgments

We thank the participants of the workshops on Heterogeneity in Host-Pathogen Systems and the members of the Collective Dynamics group at Instituto Gulbenkian de Ciéncia (IGC) for numerous discussions, particularly Erida Gjini, Joao Lopes, Caetano Souto-Maior, and Delphine Pessoa.

References

- Barskey AE, Cynthia Schulte C, Rosen JB, Handschur EF, Rausch-Phung E, et al. (2012) Mumps Outbreak in Orthodox Jewish Communities in the United States. *N Engl J Med* 367: 1704–1713.
- Aaby P, Bukh J, Lisse IM, Smiths AJ (1984) Overcrowding and intensive exposure as determinants of measles mortality. *Am J Epidemiol* 120: 49–63.
- Hornick RB, Music SI, Wenzel R, Cash R, Libonati JP, et al. (1971) The Broad Street pump revisited: Response of volunteers to ingested cholera vibrios. *Bull N Y Acad Med* 47: 1181–1191.
- Halloran ME, Longini IM Jr, Struchiner CJ (2010) *Design and Analysis of Vaccine Studies*. New York: Springer.
- Smith PG, Rodrigues LC, Fine PE (1984) Assessment of the protective efficacy of vaccines against common diseases using case-control and cohort studies. *Int J Epidemiol* 13: 87–93.
- Halloran ME, Longini IM Jr, Struchiner CJ (1996) Estimability and interpretability of vaccine efficacy using frailty mixing models. *Am J Epidemiol* 144: 83–97.
- Longini IM Jr, Halloran ME (1996) A frailty mixture model for estimating vaccine efficacy. *Appl Statist* 45: 165–173.
- Struchiner CJ, Halloran ME (2007) Randomization and baseline transmission in vaccine field trials. *Epidemiol Infect* 135: 181–194.
- Furumoto WA, Mickey R (1967) A mathematical model for the infectivity-dilution curve of tobacco mosaic virus: Theoretical consideration. *Virology* 32: 216–223.
- Furumoto WA, Mickey R (1967) A mathematical model for the infectivity-dilution curve of tobacco mosaic virus: Experimental tests. *Virology* 32: 224–233.
- Haas CN, Rose JB, Gerba CP (1999) *Quantitative Microbial Risk Assessment*. New York: John Wiley & Sons, Inc.
- Smith DL, Dushoff J, Snow RW, Hay SI (2005) The entomological inoculation rate and *Plasmodium falciparum* infection in African children. *Nature* 438: 492–495.
- Gomes MGM, Aguas R, Lopes JS, Nunes MC, Rebelo C, et al. (2012) How host selection governs tuberculosis reinfection. *Proc R Soc B* 279: 2473–2478.
- Keeling MJ, Rohani P (2008) *Modeling Infectious Diseases in Humans and Animals*. New Jersey: Princeton University Press.
- Druett HA (1952) Bacterial invasion. *Nature* 170: 288.
- Ben-Ami F, Regoes RR, Ebert D (2008) A quantitative test of the relationship between parasite dose and infection probability across different host-parasite combinations. *Proc R Soc B* 275: 853–859.
- Zwart MP, Hemerik L, Cory JS, de Visser JAGM, Bianchi FJJA, et al. (2011) An experimental test of the independent action hypothesis in virus-insect pathosystems. *Proc R Soc B* 276: 2233–2242.
- Dwyer G, Elkinton JS, Buonaccorsi JP (1997) Host heterogeneity in susceptibility and disease dynamics: Tests of a mathematical model. *Am Nat* 150: 685–707.